J Mater Sci (2007) 42:1116–1121
DOI 10.1007/s10853-006-1437-1

Potential of short Si–Ti–C–O fiber-reinforced epoxy matrix composite as electromagnetic wave absorbing material

Y. Kagawa · K. Matsumura · H. Iba · Y. Imahashi

Received: 12 February 2002 / Accepted: 14 June 2006 / Published online: 12 January 2007

Abstract The effects of fiber electrical properties on electromagnetic wave absorbing potential in short Si–Ti–C–O fiber-dispersed epoxy matrix composites were studied. Six kinds of short Si–Ti–C–O fibers with different respective electrical resistivity were incorporated into an epoxy matrix and the dielectric properties of the composites in a frequency range from 1 MHz to 1 GHz were measured. The penetration depth of electromagnetic wave, which is defined as the distance to reduce 1/e of the incident electromagnetic wave power, is obtained from the measured dielectric properties. It is found that the dielectric properties of the composites are strongly dependent on the electrical resistivity of the fiber: the use of lower electrical resistivity fiber leads to a shorter penetration depth. Independent of the electrical resistivity of fiber, the penetration depth decreases with increase in the frequency. This result demonstrates the potential of the composite as a thin electromagnetic wave absorbing material.

Y. Kagawa (✉) · K. Matsumura
Research Center for Advanced Science and Technology, The University of Tokyo, 4-6-1, Komaba, Meguro-ku, Tokyo 153-8505, Japan
e-mail: kagawa@iis.u-tokyo.ac.jp

Present Address:
H. Iba
Ube Industries, Ltd., Ube, Japan

Present Address:
Y. Imahashi
Canon Inc., Tokyo, Japan

Introduction

Electromagnetic waves are now used in various environments, and especially are in demand in the fields of advanced wireless communication systems. The wireless system requires wide frequency range electromagnetic wave absorbing material as well as electromagnetic wave reflecting and transmitting materials [1–3]. Various kinds of electromagnetic wave absorbing materials have been developed, such as ferrite-dispersed polymers [4–7], carbon-dispersed polymers [8, 9] and SiC fiber-embedded polymers [10–12].

Among the existing electromagnetic wave absorbing materials, non-stoichiometric SiC-base fiber-reinforced polymer matrix composite is believed to have both mechanical and electromagnetic wave absorbing properties and can applied as a structural electromagnetic wave absorbing material [10–12]. Although studies on the SiC-base fiber-reinforced polymer matrix composites demonstrated their high potential as an absorbing material, the potential of the SiC-base fiber for electromagnetic wave absorbing material has not well examined.

It was reported that heat treatment of SiC-base Si–Ti–C–O fiber (Tyranno®, Ube Industries, Ltd., Yamaguchi, Japan) allowed production of a wide range of electrical resistivity from 10^{-3} to 10^{4} Ωm while retaining the fiber's original mechanical performance [13]. This widely variable range of fiber electrical resistivity is due to the participation of a nanometer order thick carbon rich layer near the surface, which is induced from the non-stoichiometric chemical composition of the fiber [13, 14]. However, the effect of fiber electrical properties on the electromagnetic wave absorbing potential of the

composite has not been well studied. In the present study, attention was focused on the effect of the electrical resistivity of the Si–Ti–C–O fiber on electromagnetic wave penetration depth in the short Si–Ti–C–O fiber-reinforced epoxy matrix composite.

Experimental procedure

Composite material

Six kinds of Si–Ti–CO fiber (diameter: 8.5–13 μm, Tyranno®, Ube Industries Ltd.) were used as electromagnetic wave absorbing materials. The electrical resistivity and some properties of the fibers used are listed in Table 1. All fibers had nearly the same mechanical properties except for differences in their electrical resistivity. The chemical composition of the original fiber, i.e., before heat treatment, was Ti: 0.78, C: 44, O: 21 and the remainder was Si (at %). Control of the electrical resistivity of the fiber was carried out by heat-exposure in a high purity N_2 gas atmosphere of the original fiber. The chemical composition of the fiber was known to be the same after heat exposure [15]. The electrical resistivity of the fiber had a range from 10^{-3} to 10^{4} Ωm, this change originated from the change in distribution and content of precipitated carbon near the fiber surface, especially within ~50 nm of the surface. A typical example of the distribution of C and Si concentration near the surface determined by Auger electron spectroscopy was reported elsewhere [14]. Figure 1 shows a schematic drawing of the distribution of chemical composition of the heat-exposed Si–Ti–C–O fiber. The thickness of the carbon rich layer, x_c, is defined as the distance from the fiber surface to half the difference between carbon content at the fiber center and at the surface.

The as received fiber bundle was mechanically cut into chopped fibers in which the average length was ~2.5 mm. The chopped fibers were incorporated into an epoxy matrix. The matrix epoxy employed was a clear grade epoxy resin (Epikote 828, Yuka-Shell Epoxy Corp., Tokyo, Japan). The resin was cured using 46 wt% of curing agent (Ricaside MH-700E, New Japan Chemical Co. Ltd., Osaka, Japan) and 0.13 wt% of accelerator (DBU, Sun-Apro Corp., Kyoto, Japan). The above three components were mixed together in ambient air. The chopped Si–Ti–C–O fibers were put into the epoxy-base mixture and mechanically mixed for about 5 min and the mixture was degassed in a vacuum of 10^{-2} Pa for 1 h. Detailed processing of the epoxy mixture was reported elsewhere [16].

The mixture was poured into a Teflon®-coated tray and slightly pressed, then cured at 373 K for 4 h in ambient air using an oven. After curing, the composite

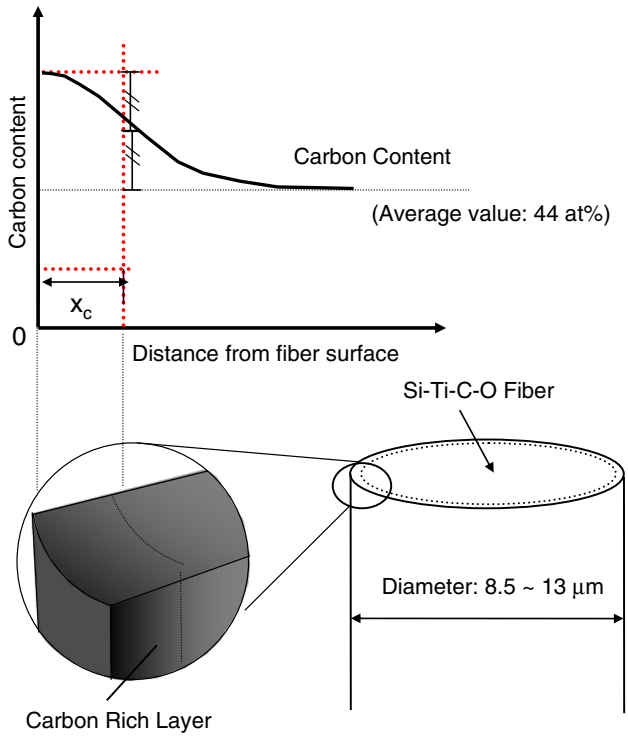

Fig. 1 Schematic drawing of the distribution of precipitated carbon in Si–Ti–C–O fiber and definition of the carbon rich layer

Table 1 Properties of the Si–Ti–C–O fibers

Properties	Fiber					
	A	B	C	D	E	F
Fiber diameter (μm)	8.5	8.5	8.5	11	11	13
Density (g/cm^3)	2.27	2.35	2.39	2.46	2.48	2.55
Thickness of carbon rich layer, X_c (nm)	0	1	7	15	20	27
Electrical resistivity, ρ_f (Ωm)	1.5×10^{4}	1.3×10^{1}	4.5×10^{-1}	5.2×10^{-2}	2.0×10^{-2}	6.5×10^{-3}
Young's modulus (GPa)	162	170	168	192	198	224
Tensile strength (GPa)	3.00	2.93	2.72	3.21	3.27	3.10

The definition of carbon rich layer thickness is shown in Fig. 1

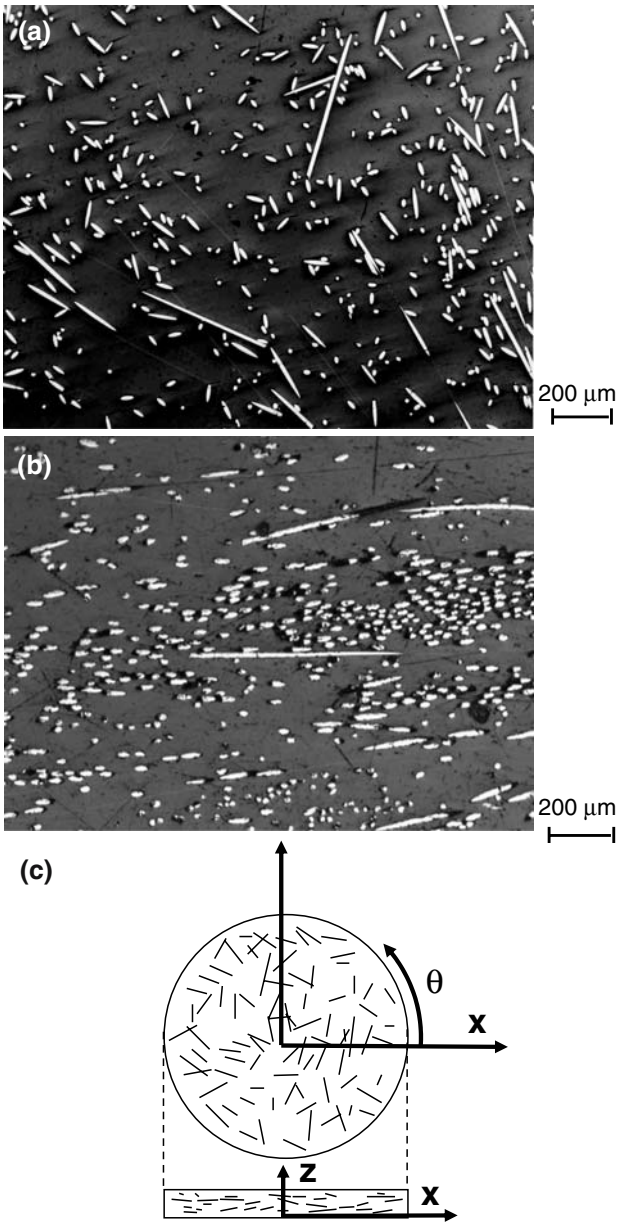

Fig. 2 Examples of the polished sections of the composite; (**a**) parallel plane, (**b**) through-the-thickness plane, and (**c**) schematic drawing of fiber distribution with definition of coordinates

was allowed to cool in the oven at a natural rate. The volume fraction of fiber was controlled by weighing the fiber before mixing, knowing the density of the fiber and the matrix after curing. The fiber volume fraction was fixed at 0.05. Figure 2 is examples of the polished sections of the composite perpendicular (a) (r–θ plane) and parallel (b) (r–z plane) to through-the-thickness plane. Detailed observation of the polished section shows that the chopped fibers were quasi-two dimensional in-plane imhomogeneously oriented in the epoxy matrix, as schematically shown in Fig. 2c. The definition of coordinate is also shown in Fig. 2c. It was found that the fiber distribution was nearly the same at any fiber electrical resistivity.

Dielectric properties and electrical resistivity

As fabricated composites were cut into disk-shaped samples using an ultrasonic machining process. The prepared samples were 12 mm in diameter and 1 mm thick. The parallel surfaces of the sample were polished to 0.5 μm with a diamond paste finish to provide a mirror surface, cleaned and dried completely by air blowing. Thereafter, a thin Au coating (~0.2 μm) was applied to both parallel surfaces by a vacuum sputtering process. This Au coating allowed good electrical connection between the fixture for dielectric measurement and the composite specimen.

The electrical resistivity of the Au-coated composite in the through-the-thickness plane was measured by a four probe method with a constant DC current ~0.1 mA at randomly selected points. Dielectric properties of the composites were measured using broad dielectric spectroscopy (Novocontrol GmβH, Hundsangen, Germany). The measurement was done in ambient air at room temperature (297 K), and measured frequency range was from 1 MHz to 1 GHz. Relative dielectric constant, ε_r', relative dielectric loss factor, ε_r'', and electrical resistivity, ρ_c, of the composites were measured at the same time.

Results and discussion

Dielectric properties of composites

Figure 3 shows examples of frequency dependence of the dielectric constant, ε_r', and the dielectric loss, ε_r'', of the composites with the electrical resistivity of the Si–Ti–C–O fibers. The dielectric constants and losses show different frequency dependence according to the electrical resistivity of the Si–Ti–C–O fiber used. This dependence becomes more remarkable with decrease in the electrical resistivity of the Si–Ti–C–O fiber. When the electrical resistivity of the fiber is as high as $\rho_f = 1.5 \times 10^4$ Ωm, the dielectric constant shows only slight frequency dependence. This suggests that the composite with low electrical resistivity fiber gives higher dielectric constant and dielectric loss compared to those with higher electrical resistivity of the fiber at the same frequency. The maximum dielectric constant and dielectric loss of the composite, respectively, are an order of ~10^2 and ~10^3, indicating that the change of electrical resistivity of the Si–Ti–C–O fiber is effective

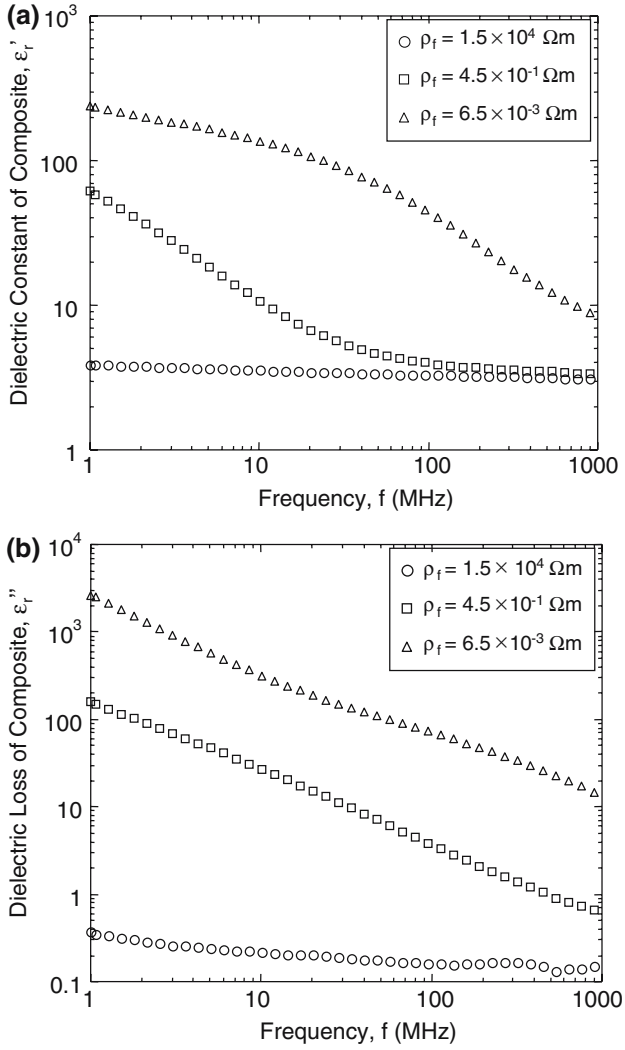

Fig. 3 (**a**) Frequency dependence of the dielectric constant, ε_r', of the composites with the electrical resistivity, ρ_f, of the Si–Ti–C–O fiber. (**b**) Frequency dependence of the dielectric loss, ε_r'', of the composites with the electrical resistivity, ρ_f, of the Si–Ti–C–O fiber

way for controlling the dielectric constant and dielectric loss of the composite in wide range.

The frequency dependence of the electrical resistivity of the composites is shown in Fig. 4. Like the frequency dependence of ε_r' and ε_r'', the electrical resistivities of all the composites tend to decrease with the increase in frequency. At the same frequency, the electrical resistivity of the composite tends to decrease with decrease in the electrical resistivity of the Si–Ti–C–O fiber. When the conductive fillers are incorporated into an insulating matrix, electrical resistivity of the composite is known to change over a wide range by the percolation effect [17, 18]. Since the epoxy matrix has a very high electrical resistivity (>10^{10} Ωm at DC [19]), this behavior obviously originates from the percolation effect among the

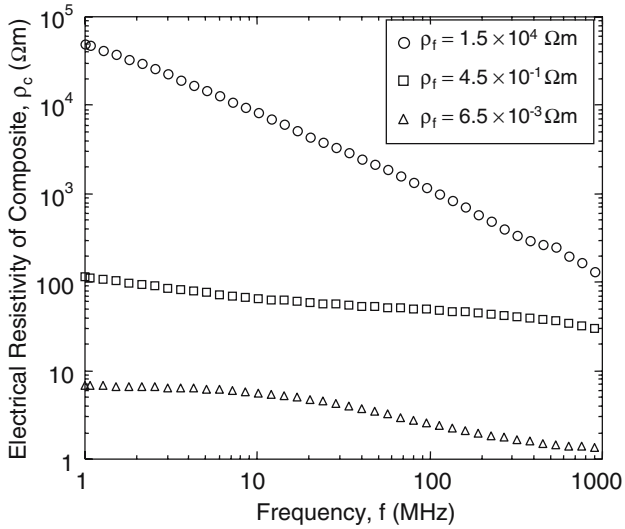

Fig. 4 The frequency dependence of the electrical resistivity of the short Si–Ti–C–O fiber-reinforced epoxy matrix composites, ρ_c

fibers, i.e. direct touching of the fiber to fiber in the epoxy matrix [20].

Electromagnetic wave absolving potential

Electromagnetic wave absorbing properties of the composites were evaluated using penetration depth of the electromagnetic wave from the surface of the composite material. Assuming that the composite is a homogeneous and isotropic material[1], the electric field, $E(x)$, as a function of depth from the surface, x, under incident amplitude of electric field, E_0, is given by [21]

$$E(x) = E_0 exp(-\alpha_c x) exp\{j(2\pi ft - \beta x)\} \quad (1)$$

where β is the phase constant, j is the complex operator, t is the time, and α_c is the attenuation constant given by [21]

$$\alpha_c = \frac{\pi f}{c}\left\{2\left(\sqrt{\varepsilon_r'^2 + \varepsilon_r''^2} - \varepsilon_r'\right)\right\}^{1/2} \quad (2)$$

Here, c is the velocity of electromagnetic wave in vacuum (3.0×10^8 m/s [22]). From Eq. (2), it is clear that larger dielectric constant, ε', and dielectric loss, ε'', give larger attenuation constant, and therefore, the

[1] In the present composite, the fiber is distributed quasi two-dimensionally in-plane random-oriented and therefore the anisotropic property should be considered in the calculation. However, the article deals with only through-the-thickness direction, and therefore, Eqs. (1) and (2) give approximate values. The error associated with this assumption is neglected in this paper.

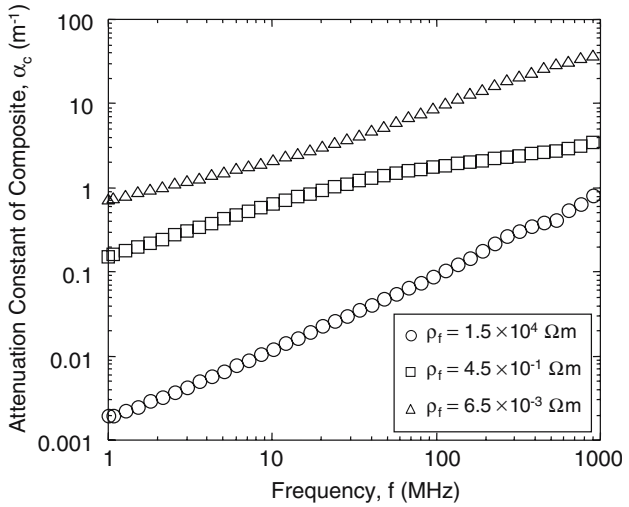

Fig. 5 Plots of the attenuation constant of the composite, α_c, and frequency, f, for the composite with the electrical resistivity of the Si–Ti–C–O fiber, ρ_f. Attenuation constant, α_c, is calculated from the Eq. (2)

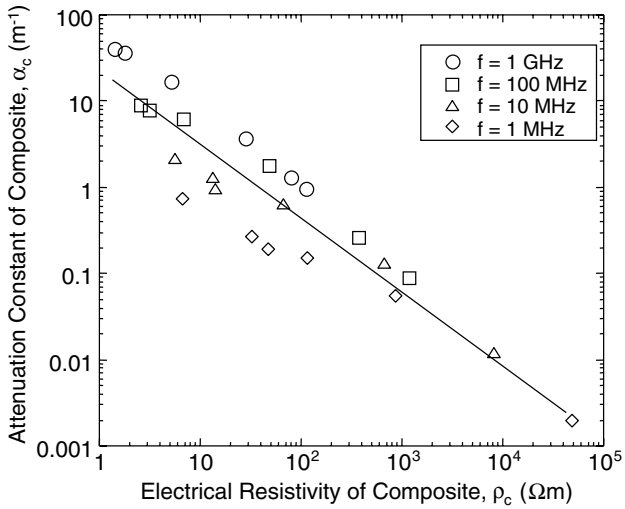

Fig. 6 Electrical resistivity dependence of the attenuation constant for frequencies 1, 10, 100 MHz and 1 GHz

discussion hereafter is focused on the composite with the highest ε_r' and ε_r'', i.e., the penetration depth using Si–Ti–C–O fiber with a lower electrical resistivity ($\rho_f = 2.0 \times 10^{-2}$ and 6.5×10^{-3} Ωm).

Figure 5 is plots of the attenuation constant of the composite, α_c, versus the frequency, f, for the composite with the electrical resistivity of the Si–Ti–C–O fiber. The attenuation constant is obtained from Eq. (2) using measured frequency dependence of dielectric properties. Figure 5 demonstrates that the attenuation constant of the composite, α_c, increases with increase in frequency and this dependency is observed independently of the electrical resistivity of the fiber, ρ_f. The dependence of the attenuation constant on the electrical resistivity of the six kinds of composites for frequencies of 1, 10, 100 MHz and 1 GHz are shown in Fig. 6. It is clear that the attenuation constant increases with decrease in electrical resistivity of the composite, which is observed independently of the frequency range. This suggests that the fiber with lower electrical resistivity gives a higher attenuation value. Using the estimated attenuation constant, α_c, the penetration depth of the electromagnetic wave to reduce its energy to 1/e is defined as $x_{1/e}$ and the value is given by

$$x_{1/e} = 1/\alpha_c \tag{3}$$

Figure 7 shows the penetration depth of electromagnetic wave for the composites obtained from Eq. (3). The penetration depths for all the measured frequency ranges decrease with the decrease in electrical resistivity of fiber as expected from Fig. 6. Within the same fiber electrical resistivity the penetration depth decreases with the increase in frequency. This experimental result suggests that Si–Ti–C–O fiber-reinforced epoxy matrix composites have suitable electromagnetic wave absorbing potential within the present frequency range, and that the material is suitable for a high frequency region.

Conclusion

The effects of electrical resistivity of the Si–Ti–C–O fiber on dielectric properties and electromagnetic wave

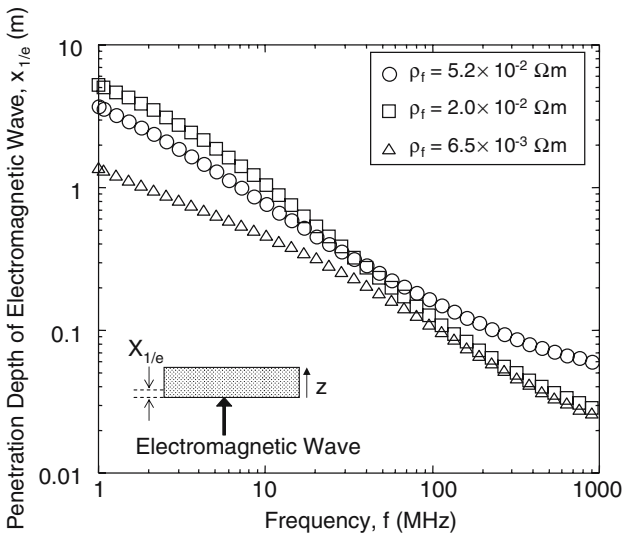

Fig. 7 Plots of penetration depth, $x_{1/e}$, of composite with the electrical resistivity, ρ_f, of the Si–Ti–C–O fiber versus frequency, f

penetration depth of in-plane random-oriented short Si–Ti–C–O fiber-reinforced epoxy matrix composites were studied. Dielectric properties of the composites were measured in frequencies from 1 MHz to 1 GHz and the penetration depth of electromagnetic wave for the composites was estimated from the dielectric properties of the composites.

The result demonstrated that these dielectric properties are strongly dependent on the electrical resistivity of the dispersed Si–Ti–C–O fiber. The penetration depth became thinner with decrease in electrical resistivity of the fiber and with increase in frequency, respectively.

Acknowledgements The work was carried out under a grant from the Ministry of Education, Science, Culture, Sports, Science and Technology of Japan. The Si–Ti–C–O fiber was supplied by Ube Industries Ltd., Ube, Japan

References

1. Shimizu Y, Suetake K (1970) Trans IEICE 53-B:143
2. Severin H (1974) IRE Trans Antennas Propagation AP–22:799
3. Tuley MT (1990) In: Radar cross section reduction short course notes. Georgia Institute of Technology
4. Naito Y, Suetake K, Fujiwara E, Sato M (1969) Trans IEICE 52–B:242
5. Hatakeyama M, Inui T (1984) IEEE Trans Magn 20:1261
6. Amin MB, James RJ (1991) The Radio and Electronic Engineer 51:209
7. Naito Y, Anzai H, Mizumoto T (1994) Trans IEICE J77-B-2:557
8. Shimizu Y, Hishikata A, Suzuki S (1985) Trans IEICE J68-B:928
9. Hashimoto O, Soh T (1991) Trans IEICE J74-B-2:563
10. Hashimoto O, Hara Y (1990) Trans IEICE J73-B-2:480
11. Hashimoto O, Sakai K (1992) Trans IEICE J75-B-2:599
12. Hashimoto O (1993) Trans IEICE J76-B-2:725
13. Shibuya M, Kajii S, Yamamura T (1993) In: Proceedings of the 3rd Japan International SAMPE Symposium. The society of material research, p 491
14. Mamiya T, Kagawa Y, Shioji Y, Sato M, Yamamura T (2000) J Am Ceram Soc 83:433
15. Ube industries, Ltd., private communication
16. Nagamuma T, Iba H, Kagawa Y (1999) J Mater Sci Lett 18:1587
17. Aharoni SM (1972) J Appl Phys 43:2463
18. Bueche F (1972) J Appl Phys 43:4837
19. Callister WD Jr (2000) In: Materials science and engineering, 5th edn. John Wiley & Sons, Inc., New York
20. Balberg I (1987) Philos Mag B 56:991
21. Von Hipper AR (1954) In: Dielectrics and waves. John Wiley & Sons, Inc., London
22. Born M, Wolf E (1980) In: Principle of optics, 6th edn. Pergamon Press, Oxford